

# Netrin (UNC-6) mediates dendritic self-avoidance

Cody J Smith<sup>1</sup>, Joseph D Watson<sup>1-3,7</sup>, Miri K VanHoven<sup>4</sup>, Daniel A Colón-Ramos<sup>5,6</sup> & David M Miller III<sup>1-3</sup>

Dendrites from a single neuron may be highly branched but typically do not overlap. Self-avoidance behavior has been shown to depend on cell-specific membrane proteins that trigger mutual repulsion. Here we report the unexpected discovery that a diffusible cue, the axon guidance protein UNC-6 (Netrin), is required for self-avoidance of sister dendrites from the PVD nociceptive neuron in *Caenorhabditis elegans*. We used time-lapse imaging to show that dendrites fail to withdraw upon mutual contact in the absence of UNC-6 signaling. We propose a model in which the UNC-40 (Deleted in Colorectal Cancer; DCC) receptor captures UNC-6 at the tips of growing dendrites for interaction with UNC-5 on the apposing branch to induce mutual repulsion. UNC-40 also responds to dendritic contact through another pathway that is independent of UNC-6. Our findings offer a new model for how an evolutionarily conserved morphogenic cue and its cognate receptors can pattern a fundamental feature of dendritic architecture.

Sensory neurons form highly branched networks of dendritic processes. Despite the complexity of these structures, dendrites arising from a given neuron rarely overlap. This phenomenon of self-avoidance is widely observed and is presumed to serve to maximize coverage of the receptive field<sup>1-3</sup>. Studies in *Drosophila melanogaster* have revealed that the cell surface proteins Dscam, Turtle and Flamingo can mediate self-avoidance and thus suggest that physical contact between sister dendrites is sufficient to trigger mutual repulsion<sup>4-8</sup>. Differential expression of the many available Dscam isoforms offers an elegant solution to the problem of distinguishing self from non-self by providing unique combinations of markers for specific neuron types. A much smaller array of distinct Dscam isoforms is produced in mammals, however, and thus is unlikely to account for the majority of self-avoidance decisions in vertebrate neural development<sup>9</sup>. Overall, the molecular roles of other determinants of dendritic architecture are also poorly understood<sup>3</sup>.

In contrast, the outgrowth of axons has been linked to a wide array of guidance cues and receptors. For example, the extracellular protein Netrin is secreted from specific donor cells to generate a graded signal that directs axon growth<sup>10-12</sup>. Netrin can also function as a short-range cue on either the membrane of the secreting cell or after capture by distal guidepost cells to direct local axon trajectory<sup>13-17</sup>. The axon guidance function of Netrin is evolutionarily conserved and depends on interaction with specific receptor proteins including UNC-40 (DCC) and UNC-5 (refs. 18,19). Here we exploit the morphological simplicity of the PVD nociceptive neuron<sup>20-23</sup> in the model organism *C. elegans* and its accessibility to live cell imaging to detect a new function for UNC-6 (Netrin) in dendritic self-avoidance. We also show that this mechanism depends on physical contact between sister dendrites. Our finding provides the first example of a diffusible cue in this role and therefore expands the repertoire of potential

self-avoidance components to include other established extracellular signaling molecules and the pathways that they control.

## RESULTS PVD neurons exhibit dendritic self-avoidance

PVD neurons display a highly branched network of sensory processes in which a collection of dendritic trees, or 'menorahs', is rooted in a common primary (1°) dendrite (Fig. 1a,b)<sup>20-22,24</sup>. This well-ordered and non-overlapping array of PVD dendrites is generated by a combination of defined branching events and an error correction mechanism in which sister dendrites are repelled by mutual contact<sup>20,22</sup>. The patterning role of self-avoidance is evident in the outgrowth of tertiary (3°) dendrites. In each menorah, paired 3° dendrites project along a sublateral nerve cord in either an anterior or posterior direction (Fig. 1a,b). We used time-lapse imaging to establish that growth continues until the tip of one 3° dendrite contacts another 3° branch pointing in the opposite direction<sup>20</sup>. Touch evoked rapid withdrawal that resulted in an eventual gap between 3° dendrites from adjacent menorahs. This mechanism readily accounts for the observation that the inter-tip gap distance was constant between flanking 3° dendrites but that adult branch length and termination points were highly variable for PVD neurons in different individuals (Fig. 1c).

As a further test of a self-avoidance model, we used a mutant of the EGL-46 (Nerfin) zinc finger transcription factor to reduce the overall number of PVD menorahs<sup>20</sup>. This genetic background effectively widens the spacing between the branch initiation points of adjacent 3° dendrites (Fig. 1d). Thus, this approach uses a genetic strategy to answer the question: if repulsion specifies the regular layout of PVD dendrites, what is the consequence of branch ablation? Our results showed that 3° branches were significantly longer in the *egl-46* mutant but that the inter-tip gap was maintained (Fig. 1e). Thus, these

<sup>1</sup>Department of Cell and Developmental Biology, Vanderbilt University, Nashville, Tennessee, USA. <sup>2</sup>Neuroscience Program, Vanderbilt University, Nashville, Tennessee, USA. <sup>3</sup>Vanderbilt Kennedy Center, Vanderbilt University, Nashville, Tennessee, USA. <sup>4</sup>Department of Biological Sciences, San Jose State University, San Jose, California, USA. <sup>5</sup>Department of Cell Biology, Yale University, New Haven, Connecticut, USA. <sup>6</sup>Program in Cellular Neuroscience and Neurodegeneration and Repair, Yale University, New Haven, Connecticut, USA. <sup>7</sup>Present address: Department of Biochemistry and Biophysics, The University of North Carolina, Chapel Hill, North Carolina, USA. Correspondence should be addressed to D.M.M. (david.miller@vanderbilt.edu).

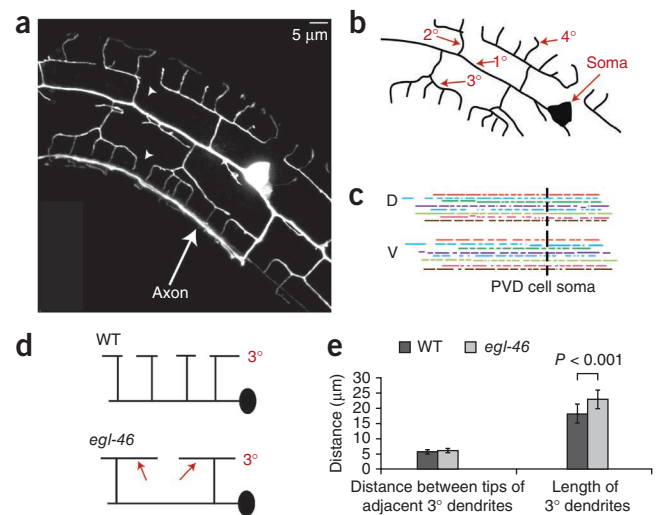
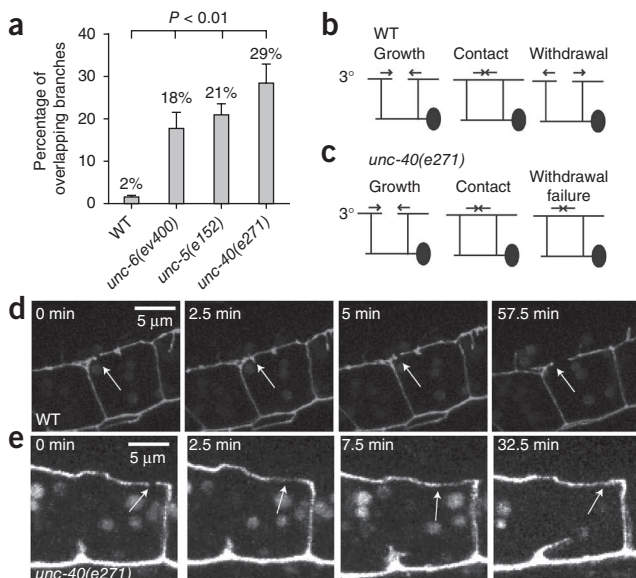
Received 9 December 2011; accepted 10 February 2012; published online 18 March 2012; doi:10.1038/nn.3065

**Figure 1** UNC-6 signaling is required for contact-dependent self-avoidance. (a) Fluorescence image of PVD neuron labeled with GFP to show the non-overlapping pattern of PVD dendrites. Arrowheads denote gaps between 3° dendrites of adjacent menorahs. The single PVD axon (arrow) marks the ventral nerve cord. (b) Tracing of PVD branches to show numbering scheme. (c) Tracings of 3° dendrites from dorsal (D) and ventral (V) regions of ten individual PVD neurons, denoted with matching colors. The 3° dendrites do not terminate at specific anatomical regions or show a single length, as would be expected if outgrowth were governed by external landmarks or limited by an intrinsic mechanism of length determination. (d) *egl-46* mutants show fewer 2° branches and longer 3° dendrites (arrows). (e) PVD neurons have fewer 2° branches in *egl-46*(n1076) mutants ( $32.3 \pm 5.3$ ) than wild type (WT) ( $38.9 \pm 5.4$ ). Despite the consequent reduction in the overall number of 3° branches in *egl-46* mutants, the normal distance between the tips of adjacent 3° dendrites is maintained by extending the average outgrowth length of 3° dendrites. Error bars, s.e.m.

observations rule out models in which branch length is determined by a fixed yardstick or defined by external landmarks but favor the idea that the non-overlapping PVD dendritic architecture is achieved through a contact-dependent mechanism of self-recognition.

### UNC-6 signaling is required for dendritic self-avoidance

We generated a PVD expression profile<sup>20</sup> and used genetic analysis of known axon guidance molecules suggested by this list to test for potential roles in dendritic morphogenesis (Supplementary Table 1). We noted that genetic ablation of the UNC-6 receptors UNC-40 and UNC-5 altered several aspects of PVD morphology (Supplementary Fig. 1; refs. 20,24). One result was the aberrant occurrence of overlaps between flanking menorahs in the adult (Fig. 2a). We used time-lapse imaging to establish that this mutant phenotype arises from a self-avoidance defect. In the wild type, 3° dendrites from adjacent menorahs grew toward each other but quickly retracted, with >50% regressing within 3 min of contact and <13% still touching at the 10-min mark; ultimately, less than 2% of wild-type 3° dendrites overlapped with each other (Fig. 2, Supplementary Movie 1 and Supplementary Fig. 2). In contrast, in *unc-40*(e271) mutants, 76% of adjacent 3° dendrites failed to withdraw within 10 min of contact and almost one-third (29%) never regressed (Fig. 2a,c,e) (Supplementary Movie 2 and Supplementary Fig. 2). Similar defects were captured in time-lapse movies of *unc-5*(e152) mutants (Supplementary Movie 3 and Supplementary Fig. 2).



Motivated by these results, we examined the mutant *unc-6*(ev400) and detected 3° dendrite self-avoidance defects resembling those of *unc-40* and *unc-5* mutants (Fig. 2a). If these genes function in a common pathway, double mutants between *unc-6* and each of its receptors should fail to enhance the self-avoidance defect of either single mutant. This prediction was confirmed for the self-avoidance defect arising from the combination of *unc-5* and *unc-6*, which was comparable to that of either *unc-5* or *unc-6* alone (Supplementary Fig. 3). However, the *unc-40* mutation enhanced both the *unc-5* and *unc-6* single mutant self-avoidance phenotypes. These results are consistent with a model in which *unc-40* exercises a role in self-avoidance that is independent of *unc-6* signaling through *unc-5*. In addition, because neither *unc-5* nor *unc-6* enhanced the *unc-40* self-avoidance defect (Supplementary Fig. 3), we conclude that *unc-40* also functions in the *unc-6*- and *unc-5*-dependent pathway. Here we describe experiments designed to establish the mechanism whereby UNC-6 and its receptors, UNC-40 and UNC-5, mediate dendritic self-avoidance.

### Self-avoidance requires UNC-6 but not a graded UNC-6 signal

UNC-6 is secreted from ventral cells to direct axonal outgrowth and cell migration along the dorso-ventral body axis<sup>10,25</sup>. When this ventral source of UNC-6 was removed, in *unc-6*(ev400) mutants, 18% of PVD 3° branches overlapped (Fig. 3). This defect was complemented by UNC-6 expression with the native *unc-6* promoter (Fig. 3d). Transgenic expression of UNC-6 in a ventral neuron (AVA) with the *rig-3* promoter<sup>26</sup> also improved the self-avoidance response (8% overlapping branches,  $P = 0.02$  versus *unc-6*), indicating that UNC-6 expression from ventrally located cells is sufficient to mediate PVD 3° branch self-avoidance (Fig. 3d).

Although extracellular UNC-6 protein is presumably distributed in a ventral to dorsal gradient, we did not observe a significant

**Figure 2** UNC-6 signaling is required for contact-dependent self-avoidance. (a) The 3° branches from adjacent menorahs overlap in *unc-6*(ev400), *unc-5*(e152) and *unc-40*(e271) mutants more frequently than in wild type (WT).  $P < 0.01$ . Error bars, s.e.m. (b) Schematic showing 3° dendrite outgrowth, contact and retraction in WT. (c) 3° branches fail to withdraw after contact in an *unc-40* mutant. (d) Images captured from a time-lapse movie showing contact and then rapid withdrawal (<2.5 min) (arrows) of 3° branches in WT. (e) Successive images showing 3° branches failing to withdraw within 30 min of mutual contact in *unc-40*(e270) (arrows).

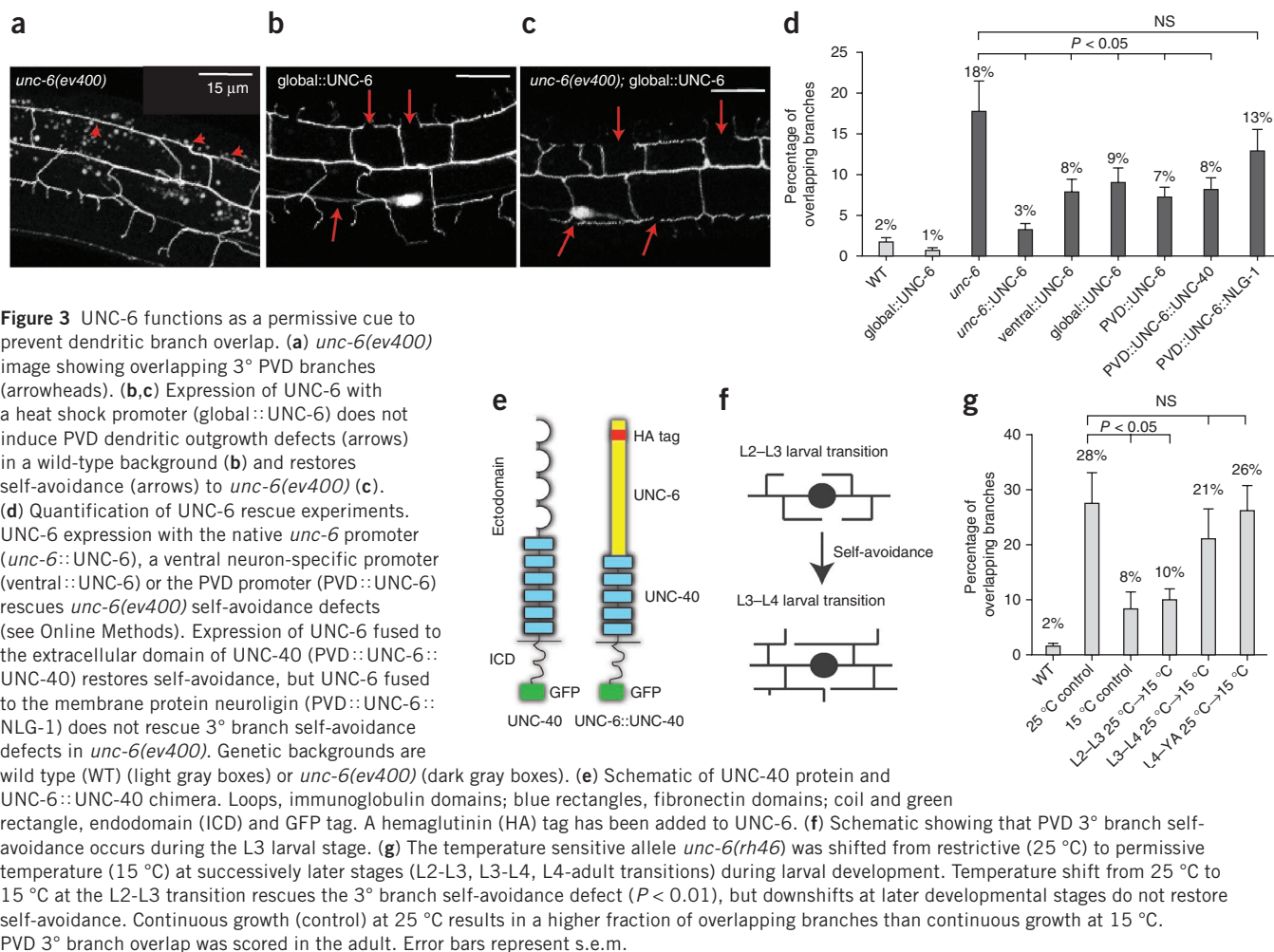


**Figure 3** UNC-6 functions as a permissive cue to prevent dendritic branch overlap. (a) *unc-6(ev400)* image showing overlapping 3° PVD branches (arrowheads). (b,c) Expression of UNC-6 with a heat shock promoter (*global*::*UNC-6*) does not induce PVD dendritic outgrowth defects (arrows) in a wild-type background (b) and restores self-avoidance (arrows) to *unc-6(ev400)* (c). (d) Quantification of UNC-6 rescue experiments. UNC-6 expression with the native *unc-6* promoter (*unc-6*::*UNC-6*), a ventral neuron-specific promoter (*ventral*::*UNC-6*) or the PVD promoter (*PVD*::*UNC-6*) rescues *unc-6(ev400)* self-avoidance defects (see Online Methods). Expression of UNC-6 fused to the extracellular domain of UNC-40 (*PVD*::*UNC-6*::*UNC-40*) restores self-avoidance, but UNC-6 fused to the membrane protein neuroligin (*PVD*::*UNC-6*::*NLG-1*) does not rescue 3° branch self-avoidance defects in *unc-6(ev400)*. Genetic backgrounds are wild type (WT) (light gray boxes) or *unc-6(ev400)* (dark gray boxes). (e) Schematic of UNC-40 protein and UNC-6::UNC-40 chimera. Loops, immunoglobulin domains; blue rectangles, fibronectin domains; coil and green rectangle, endodomain (ICD) and GFP tag. A hemagglutinin (HA) tag has been added to UNC-6. (f) Schematic showing that PVD 3° branch self-avoidance occurs during the L3 larval stage. (g) The temperature sensitive allele *unc-6(rh46)* was shifted from restrictive (25 °C) to permissive temperature (15 °C) at successively later stages (L2-L3, L3-L4, L4-adult transitions) during larval development. Temperature shift from 25 °C to 15 °C at the L2-L3 transition rescues the 3° branch self-avoidance defect ( $P < 0.01$ ), but downshifts at later developmental stages do not restore self-avoidance. Continuous growth (control) at 25 °C results in a higher fraction of overlapping branches than continuous growth at 15 °C. PVD 3° branch overlap was scored in the adult. Error bars represent s.e.m.

difference ( $P > 0.05$ ) in the extent of self-avoidance errors in ventral versus dorsal 3° branches in *unc-6(ev400)* (Supplementary Fig. 4). We next used a heat shock promoter (*hsp16.2*) to drive expression of UNC-6 in all cells<sup>27</sup> and thereby directly determine whether a ventral to dorsal gradient of UNC-6 is required for self-avoidance. Although global expression of UNC-6 is known to disrupt axon guidance along the dorso-ventral axis<sup>27</sup>, ubiquitous UNC-6 expression in a wild-type background during multiple larval stages did not perturb PVD 3° branch self-avoidance (Fig. 3b,d).

We reasoned that UNC-6 might function as a permissive cue in this case, such that a specific source or gradient of UNC-6 is not necessary provided sufficient ligand is available. This idea was substantiated by our finding that global expression of UNC-6 in *unc-6(ev400)* mutants with the heat shock promoter before the L3 larval stage rescued 3° branch self-avoidance (9% overlapping branches,  $P = 0.04$  versus *unc-6*) (Fig. 3c,d). In addition, we showed that expression of UNC-6 in PVD with the *F49H12.4* promoter<sup>28</sup> also rescued *unc-6(ev400)* self-avoidance defects (7% overlapping branches,  $P = 0.01$  versus *unc-6*) (Fig. 3d). On the basis of these results, we conclude that PVD dendritic self-avoidance is independent of the UNC-6 gradient and therefore that UNC-6 does not provide a directional signal to repel dendritic outgrowth. We considered an alternative model in which the mere availability of UNC-6 is sufficient to trigger repulsion and next asked the question of when this function is required.

**UNC-6 is required during the period when dendrites self-avoid** Time-lapse imaging established that PVD 3° branch self-avoidance occurred during the L3 larval stage<sup>20</sup>. If UNC-6 is directly involved in self-avoidance, then UNC-6 function should be required during this period. We used a conditional *unc-6* allele (*rh46*) to test this idea in temperature shift experiments that regulate temporal UNC-6 activity<sup>29</sup>.

*unc-6(rh46)* mutants grown at the restrictive temperature (25 °C) showed a self-avoidance defect (28% of overlapping 3° branches, Fig. 3g) comparable to that of the *unc-6(ev400)* null allele ( $P = 0.14$  *ev400* versus *rh46*), which suggests that the *rh46* point mutation results in a dysfunctional UNC-6 protein at restrictive temperature<sup>29</sup>. The self-avoidance defect was weaker but still significant at 15 °C (Fig. 3g, 8% of overlapping 3° branches,  $P = 0.006$  versus 25 °C control,  $P = 0.047$  versus N2), indicating that the *rh46* mutant UNC-6 protein is only partially active at permissive temperature. We shifted *unc-6(rh46)* worms from restrictive temperature (25 °C) to permissive temperature (15 °C) at succeeding developmental stages (Fig. 3f,g). *unc-6(rh46)* larvae downshifted at the L2/L3 transition and then maintained at permissive temperature until the adult showed a self-avoidance defect comparable to that of control worms grown continuously at 15 °C (Fig. 3g, 10% overlapping branches,  $P = 0.007$  versus 25 °C control). In contrast, downshifts to permissive temperature (that is, restoration of UNC-6 activity) after the L2/L3 transition resulted in a self-avoidance defect as severe as that of *unc-6(rh46)* mutants grown continuously at the restrictive temperature (Fig. 3g,

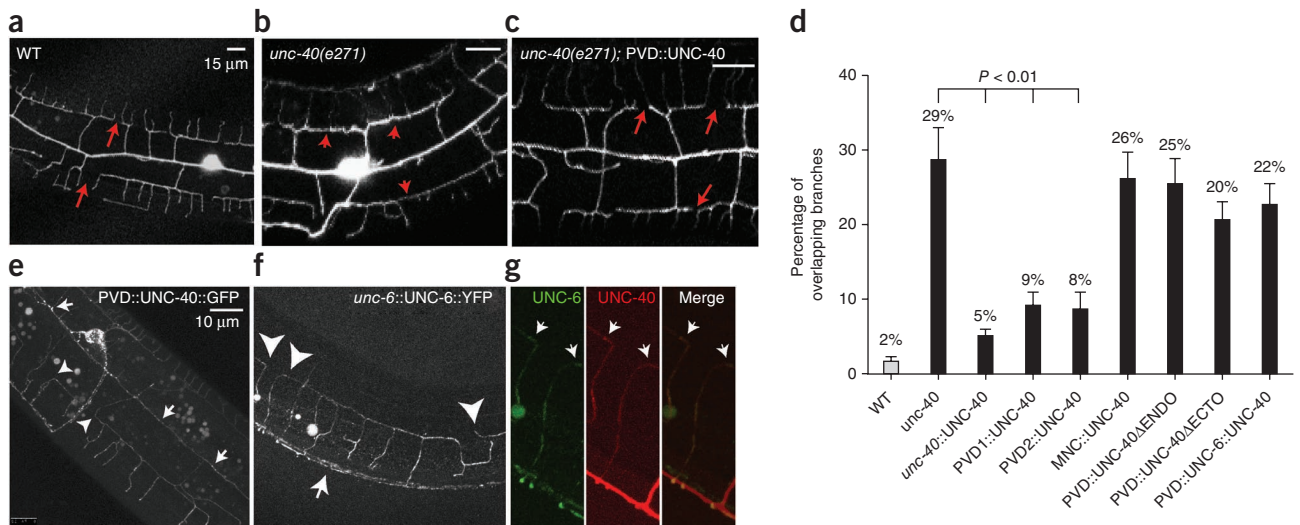


**Figure 4** UNC-40 functions in PVD to mediate self-avoidance and captures exogenous UNC-6 at the PVD cell surface. (a) PVD 3° dendrites do not overlap in wild-type (WT) adults (arrows). (b,c) Expression of UNC-40 (PVD::UNC-40) in *unc-40(e271)* rescues (arrows) the Unc-40 self-avoidance defect (arrowheads). (d) Quantification confirms that expression of UNC-40 with the native *unc-40* promoter (*unc-40::UNC-40*) or with two different PVD promoters (PVD1::UNC-40, PVD2::UNC-40) restores PVD dendritic self-avoidance, whereas expression with a motor neuron-specific promoter (MNC::UNC-40) does not. PVD expression of UNC-40 lacking either the extracellular UNC-6 binding domain (PVD::UNC-40ΔECTO) or intracellular signaling domain (PVD::UNC-40ΔENDO) does not rescue self-avoidance. Genetic backgrounds are WT (gray box) or *unc-40(e271)* (black boxes). Error bars, s.e.m. (e) PVD expression of GFP-labeled UNC-40 (PVD::UNC-40::GFP) results in GFP puncta in PVD processes (arrows) and at tips of growing dendrites (arrowheads). (f) YFP-labeled UNC-6 expressed from its native promoter in ventral cells (*unc-6::UNC-6::YFP*) decorates PVD neurons (arrowheads) expressing UNC-40::mCherry. Arrow denotes UNC-6::YFP labeling of ventral nerve cord. (g) UNC-6::YFP (UNC-6, green; left) labeling of PVD expressing UNC-40::mCherry (UNC-40, red; center). Merged image shows colocalization of UNC-6::YFP and UNC-40::mCherry puncta (arrows).

$P = 0.42$  for L3/L4,  $P = 0.86$  for L4/young adult versus 25 °C control). These results indicate that self-avoidance does not depend on UNC-6 function during embryonic and early larval development but that UNC-6 is required after the beginning of the L3 stage.

Similar temperature upshift experiments confirmed that loss of UNC-6 function during the L3 larval period enhanced the *rh46* self-avoidance defect, but later shifts to restrictive temperature after 3° branch outgrowth was complete (that is, L3/L4 or L4/young adult) did not result in a severe branch overlap phenotype (Supplementary Fig. 5). Thus, our results are consistent with a model in which UNC-6 function is required for self-avoidance during a brief developmental window in the L3 larval stage in which 3° dendrites actively engage in outgrowth and contact-dependent repulsion. This finding argues against the possibility that UNC-6 signaling fulfills an earlier, indirect role in which it primes PVD dendrites for self-avoidance by regulating expression<sup>30</sup>, for example, of an alternative set of interacting components.

#### UNC-40 and UNC-5 function cell-autonomously in PVD

Genetic ablation of UNC-5 and UNC-40 resulted in significant overlap of 3° dendrites (Fig. 2a). Because UNC-5 and UNC-40 have been previously shown to function as receptors for UNC-6 (refs. 10,18,19) and because UNC-5 and UNC-40 transcripts were enriched in our PVD microarray data set<sup>20</sup>, we reasoned that UNC-5 and UNC-40 are likely to act in PVD to prevent overlap of 3° dendrites. This model predicts that expression of UNC-5 and UNC-40 in PVD should be sufficient to restore self-avoidance to the corresponding *unc-5* or *unc-40* mutants.

Expression of UNC-40 with its endogenous promoter in *unc-40(e271)* mutants reduced the frequency of overlapping branches from 29% to 5% ( $P = 3 \times 10^{-5}$  versus *unc-40*) (Fig. 4). UNC-40 expression with the PVD promoters *F49H12.4* (ref. 28) or *ser2prom3* (ref. 31) also showed significant rescue (8% overlapping 3° branches,  $P = 5 \times 10^{-7}$  versus *unc-40*) (Fig. 4c,d). Thus, these results indicate a cell-autonomous function of UNC-40 in PVD.

We have previously noted that a substantial fraction of PVD 2° branches fasciculate with motor neuron commissures that also project from the ventral to dorsal side of the worm<sup>20</sup>. To determine whether PVD dendritic self-avoidance is indirectly compromised by commissural axon guidance defects in *unc-40(e271)*<sup>18</sup>, we restored UNC-40 expression to ventral cord motor neurons with the *unc-25* promoter<sup>32</sup>. Motor neuron expression of UNC-40 largely rescued commissural axon outgrowth to the dorsal cord, as expected<sup>18</sup> (Supplementary Fig. 6), but did not restore PVD self-avoidance (Fig. 4d).

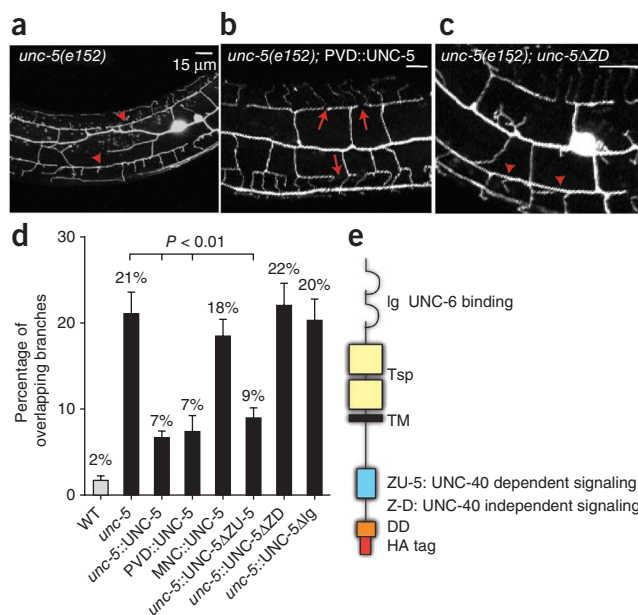
In similar experiments, expression of UNC-5 under its endogenous promoter resulted in a significantly reduced fraction of overlapping branches in the *unc-5(e152)* mutant (Fig. 5) (7%,  $P = 8.6 \times 10^{-5}$  versus *unc-5*). A cell-autonomous role for UNC-5 in PVD is consistent with our finding that UNC-5 expression with the *F49H12.4* promoter also rescued the UNC-5 self-avoidance defect (Fig. 5b,d,  $P = 1.8 \times 10^{-4}$  versus *unc-5*). Restoration of UNC-5 expression in motor neurons did not complement *unc-5(e152)* PVD self-avoidance errors (Fig. 5d) but did repair the uncoordinated phenotype that arises from misguided motor axon outgrowth (data not shown)<sup>33,34</sup>. The results of these cell-specific rescue experiments show that UNC-5 function is required in the PVD dendrites to prevent overlap of 3° branches.

#### UNC-40 localizes UNC-6 to PVD dendrites

Consistent with the hypothesis that UNC-40 function is required in PVD dendrites, PVD expression of a GFP-tagged functional UNC-40 protein (UNC-40::GFP)<sup>27</sup> resulted in distinct GFP puncta in PVD processes (Fig. 3e). Moreover, UNC-40::GFP puncta could be readily seen at the tips of 3° dendrites, where contact-dependent self-avoidance occurs (Fig. 4e,g).

We considered the possibility that UNC-6 functions as a contact-dependent repellent and tested this idea with an experiment designed to detect UNC-6 at the surface of PVD dendrites. We used the endogenous *unc-6* promoter to drive expression of UNC-6::YFP<sup>35</sup>.

**Figure 5** UNC-5 is required in PVD and uses UNC-40-independent signaling to mediate self-avoidance. (a) *unc-5(e152)* shows PVD self-avoidance defects (arrowheads). (b,c) Expression of UNC-5 with the PVD promoter (PVD::UNC-5) prevents 3° branch overlap in *unc-5(e152)* (b), whereas UNC-5 lacking the Z-D domain does not rescue (c). (d) Quantification. Expression of UNC-5 with the native *unc-5* promoter (*unc-5::UNC-5*) or with the PVD promoter (PVD::UNC-5) restores PVD self-avoidance, whereas expression of the UNC-5 with a motor neuron promoter (MNC::UNC-5) does not. Expression of UNC-5 proteins lacking either an UNC-40-independent cytoplasmic signaling domain (*unc-5::UNC-5ΔZD*) or an UNC-6-binding domain (*unc-5::UNC-5ΔIg*) does not rescue self-avoidance in *unc-5(e152)* mutants, whereas expression of an UNC-5 protein lacking an UNC-40-dependent signaling domain (*unc-5::UNC-5ΔZU-5*) does prevent 3° branch overlap. Genetic backgrounds are wild type (WT) (gray box) or *unc-5(e152)* (black boxes). Error bars, s.e.m. (e) Schematic of UNC-5 protein showing: immunoglobulin (Ig) domains; thrombospondin domains (Tsp); transmembrane domain (TM); ZU-5, Z-D (below ZU-5) and Death domain (DD) intracellular regions; and C-terminal hemagglutinin (HA) tag.



Although this transgene rescued *unc-6* axon guidance defects and therefore must yield a secreted, functional UNC-6::YFP protein, UNC-6::YFP was too diffuse to detect in the wild-type outside of the ventral cells in which it is expressed (Supplementary Fig. 7)<sup>35</sup>. To enhance the sensitivity of this assay, we labeled UNC-40 with the fluorescent protein mCherry and expressed it in PVD. In this background, UNC-6::YFP was evident as YFP puncta that overlapped with mCherry::UNC-40 (Fig. 4f,g). In contrast, expression of UNC-5 in PVD rescued the *unc-5* self-avoidance defect (Fig. 5d) but did not result in detectable localization of UNC-6::YFP on PVD (data not shown). These results are consistent with a model in which UNC-40, but not the UNC-5 receptor, captures UNC-6 from the extracellular space at the surface of PVD dendrites. This idea is supported by our finding that PVD expression of a truncated UNC-40 protein lacking the UNC-6-binding extracellular domain (PVD::UNC-40ΔECTO) did not restore 3° branch self-avoidance in *unc-40(e271)* mutants (20% overlapping dendrites,  $P = 0.23$  versus *unc-40*), whereas PVD expression of intact UNC-40 protein was sufficient (Fig. 4d). To rule out the possibility of a dominant negative effect, we determined that the PVD::UNC-40ΔECTO protein did not disrupt self-avoidance in a wild-type background (data not shown).

### UNC-6 bound to UNC-40 functions as a short-range cue

Our results show that UNC-6 secreted from a ventral source can be captured by UNC-40 at the surface of PVD dendrites. Because PVD sister dendrite repulsion depends on direct contact, we wondered whether UNC-6 bound to UNC-40 at the tips of touching 3° dendrites could trigger this response. In this model, UNC-40 might adopt a role in which it positions UNC-6 at this critical location to activate withdrawal of an apposing dendrite. This idea mirrors the observation that *Drosophila* DCC (Frazzled; Fra) can sequester exogenous NetrinB at the surface of guidepost cells to steer local axon outgrowth in a contact-dependent mechanism<sup>13</sup>.

Our model predicts that UNC-6 protein tethered to the UNC-40 receptor can function as a short-range cue. To test this idea, we fused UNC-6 to the extracellular region of UNC-40 (PVD::UNC-6::UNC-40) and expressed the chimeric protein in PVD. This membrane-bound form of UNC-6 rescued the dendritic self-avoidance defects of *unc-6(ev400)* worms (8% overlapping 3° branches,  $P = 0.02$  versus *unc-6*) (Fig. 3d). Expression in AVA interneurons in the ventral nerve cord with the *rig-3* promoter<sup>26</sup> (ventral::UNC-6::UNC-40), however, did not restore self-avoidance to *unc-6(ev400)* mutants and therefore confirmed that the UNC-6::UNC-40 fusion protein is not

released from the cell surface (Supplementary Fig. 8). Thus, our results are consistent with a model in which UNC-40 localizes exogenous UNC-6 to the surface of PVD dendrites, where it functions as a short-range cue to trigger self-avoidance. This configuration may be specifically required because PVD expression of UNC-6 fused to the N terminus of a different transmembrane protein, NLG-1 (neuroigin) (PVD::UNC-6::NLG-1)<sup>17</sup>, did not rescue self-avoidance in *unc-6(ev400)* mutants (Fig. 3d).

### Self-avoidance is mediated by UNC-5 signaling

The next problem to consider was how apposing PVD dendrites might detect this local UNC-40-bound UNC-6 ligand. Because of the well established role of UNC-5 in mediating repulsive responses to Netrins<sup>14,19,33</sup>, and our finding that UNC-5 expression in PVD was necessary for self-avoidance, we imagined that UNC-5 could provide this function. An UNC-5 protein with a mutation in the extracellular immunoglobulin domain that disrupts UNC-6 binding failed to rescue self-avoidance when expressed in *unc-5(e152)* mutants (Fig. 5d, 20% overlapping branches,  $P = 0.83$  versus *unc-5*). This finding is consistent with genetic results (Supplementary Fig. 3) showing that *unc-5* and *unc-6* function in a common pathway to mediate self-avoidance and with the proposal that UNC-6 binding to UNC-5 is necessary for this interaction. Genetic analysis in *C. elegans* has shown that UNC-5 can mediate UNC-6-dependent repulsion either in concert with UNC-40 or independently<sup>34</sup>. These UNC-5 functions depend on specific conserved cytoplasmic domains: the Z-D sequence is necessary for UNC-40-independent signaling, whereas the ZU-5 region is required for UNC-40-dependent activity<sup>34</sup>.

To distinguish between these models, we tested mutant versions of the UNC-5 protein that lacked either the Z-D region (UNC-40-independent signaling) or the ZU-5 domain (UNC-40-dependent signaling). Previous work has shown that UNC-5 localization is not disrupted by these mutations<sup>34</sup>. Transgenic expression of the UNC-5 protein lacking the Z-D domain (UNC-5ΔZD) did not restore self-avoidance to an *unc-5(e152)* mutant (Fig. 5c,d, 22% overlapping branches,  $P = 0.79$  versus *unc-5*). In contrast, deletion of the ZU-5 region (UNC-5ΔZU-5) that is required for UNC-40-dependent signaling significantly improved the frequency of self-avoidance in comparison to the *unc-5(e152)* mutant alone (Fig. 5d, 9% overlapping

branches,  $P = 3 \times 10^{-4}$ ). These results are consistent with a model in which UNC-5-mediated repulsion does not depend on interactions *in cis* with the UNC-40 protein but rather UNC-40 function is required for localizing UNC-6 for binding *in trans* to UNC-5 at the apposing tip of the adjacent 3° dendrite.

### UNC-40 signaling is required for self-avoidance

Although the UNC-6::UNC-40 fusion protein rescued the *unc-6* mutant (Fig. 3d) and therefore is likely to function as a membrane-bound cue to trigger dendrite repulsion, UNC-6:UNC-40 did not restore self-avoidance to *unc-40(e271)* mutants (Fig. 4d). One explanation for this result is that *unc-40* signaling is not active in the UNC-6::UNC-40 fusion protein and that this UNC-40 function is necessary for self-avoidance.

We tested this idea with a modified UNC-40 protein that lacked the intracellular domain (ICD) that mediates UNC-40 downstream signaling<sup>36,37</sup>. Notably, PVD expression of this truncated UNC-40 protein (PVD::UNC-40ΔENDO) in *unc-40(e271)* mutants did not rescue dendrite repulsion (Fig. 4d). Thus, our results indicate that UNC-40 provides the dual roles of capturing UNC-6 at the PVD cell surface for interaction with UNC-5 as well as activating a downstream pathway to mediate self-avoidance.

### DISCUSSION

Dendrites from a single neuron may be highly branched but rarely touch one another<sup>2,9</sup>. The absence of overlap arises from a mechanism in which sister dendrites are mutually repelled by transient encounters during outgrowth. The necessity of physical contact for self-avoidance is indicative of interaction between surface markers that trigger repulsion<sup>2</sup>. This model is substantiated by the recent discovery that membrane proteins can mediate self-avoidance in *Drosophila* sensory neurons<sup>5–8</sup>. Here we describe a new mechanism in the nematode, *C. elegans*, in which this self-recognition function is provided by a diffusible cue (Supplementary Fig. 9).

Our results show that UNC-6 (Netrin) is secreted from ventral cells to modulate self-avoidance of PVD sensory neuron dendrites in distal, lateral locations. We propose that UNC-6 is sequestered at the surface of PVD dendritic branches by the canonical receptor UNC-40 (DCC) where it is positioned to trigger a repulsive response on contact with UNC-5 on the apposing dendrite. PVD self-avoidance also depends on UNC-40 function in a separate pathway that does not require *unc-5* and *unc-6* (Supplementary Fig. 9).

In some respects, our model parallels an earlier finding in which *Drosophila* DCC (Frazzled) functions in guidepost cells to capture Netrin as a local guidance cue for nearby axons<sup>13,38,39</sup>. In this setting, however, the Netrin receptor in the responding cells is unknown and this signaling event occurs between separate cells. In the model that we have proposed, UNC-5 mediates a negative response to UNC-6 (Netrin) between spatially distinct membrane regions of the same cell. Netrin has also been shown to function as a short-range signal for axonal and dendritic guidance in other contexts and for defining the placement of synapses between specific neurons<sup>14–17</sup>. The phenomenon of self-avoidance that we have detected includes additional features that point to a complex mechanism. In addition to the proposed role for UNC-40 of sequestering UNC-6 for interaction with UNC-5, our genetic evidence (Supplementary Fig. 3) indicates that UNC-40 also functions in a parallel self-avoidance pathway that does not involve *unc-5* and *unc-6*. UNC-6-independent signaling by UNC-40 has been previously observed<sup>18,30,40</sup> and is suggestive of additional UNC-40 activating ligands. Previous work has shown that UNC-5 and DCC can signal independently of each other to mediate repulsion to Netrins<sup>14,18,41,42</sup>,

but our findings include the additional observation that this activity requires physical contact between apposing dendrites.

In addition to expanding the repertoire of self-avoidance proteins, our discovery that UNC-40 and UNC-5 are involved suggests that other established Netrin signaling proteins could also be used to trigger repulsion. For example, we note that the UNC-6 pathway components UNC-34 (Ena), CED-10 (Rac) and MIG-10 (lamellipodin)<sup>43–45</sup> are highly expressed in PVD and therefore available for this role<sup>20</sup>. The significance of this possibility is underscored by the lack of knowledge of the downstream mechanisms that reorganize the dendritic cytoskeleton to effect mutual repulsion<sup>46</sup>. For example, the intracellular proteins tricornered (*trc*) and furry (*fry*) are required for dendritic self-avoidance in a subset of *Drosophila* sensory neurons, but mechanisms that activate these components are poorly defined<sup>7,47</sup>. In addition, the cytoplasmic domain of Dscam is necessary for self-avoidance, but no downstream effectors have been identified<sup>6</sup>.

We have established that UNC-6 is required for self-avoidance of PVD dendrites. However, our results also point to additional mechanisms for regulating isoneuronal repulsion. We note that most (~65%) of PVD 3° dendrites undergo normal self-avoidance in strong loss-of-function alleles of UNC-6 pathway genes (Fig. 2). This result parallels the observation that mutants in self-avoidance genes in *Drosophila* (for example, Dscam, Turtle) and *C. elegans* (for example, *eff-1*) are also incompletely penetrant<sup>6,8,22</sup>.

Although our results reveal a new role for Netrin signaling in dendritic self-avoidance, the model that we have proposed involving a single cue and its receptors is unlikely to provide a general solution to the problem that individual neurons face of distinguishing self from non-self. The cell surface markers Dscam and protocadherins, which can be expressed in many alternative forms, are proposed to fulfill this role by providing unique combinations of labels for marking single neuron types in complex neural environments<sup>9</sup>. However, our discovery of a mechanism whereby an exogenous cue can be used to pattern dendritic self-avoidance suggests that other extracellular signals and their receptors could be similarly employed. This possibility significantly expands the potential utility of this self-avoidance strategy.

### METHODS

Methods and any associated references are available in the online version of the paper at <http://www.nature.com/natureneuroscience/>.

Note: Supplementary information is available on the Nature Neuroscience website.

### ACKNOWLEDGMENTS

We thank C. Bargmann (Rockefeller University) for *unc-86::UNC-40::GFP*, *hsp16.2::UNC-6::HA* and the CX6488 strain; W. Wadsworth (Rutgers University) for the pIM97 *unc-6* expression construct and *unc-6(rh46)*; K. Shen (Stanford University) for constructs used to make pCJS01, *F49H12.4::gateway::mcherry*; P. Roy (University of Toronto) for the *unc-40(e271)* sequence; Y. Goshima (Yokohama City University) for *ghIs9*; J. Culotti (Mount Sinai Hospital, Toronto) for the *unc-5* rescue construct and for the modified UNC-5 protein strains used for structure–function analysis and members of the D.M.M., R.B. and D.A.C.-R. laboratories for technical advice and for comments on the manuscript. Some of the strains used in this work were provided by the *C. elegans* Genetics Center, which is supported by the US National Institutes of Health (NIH) National Center for Research Resources. This work was supported by NIH R01 NS26115 (D.M.M.), NIH R21 NS06882 (D.M.M.), NIH F31 NS071801 (C.J.S.), NIH R00 NS057931 (D.A.C.-R.), the Klingenstein Foundation and an Alfred P. Sloan Foundation fellowship (D.A.C.-R.), and NIH MBRS SC3 GM089595 (M.K.V.).

### AUTHOR CONTRIBUTIONS

C.J.S. and D.M.M. designed the experiments. C.J.S. performed experiments with advice from D.M.M. J.D.W. helped with the phenotypic analysis of UNC-6 signaling mutants. D.A.C.-R. and M.K.V. provided reagents to test the cell-specific requirement of UNC-40 and UNC-6 and provided advice. C.J.S. and D.M.M. wrote the paper with input from coauthors.

## COMPETING FINANCIAL INTERESTS

The authors declare no competing financial interests.

Published online at <http://www.nature.com/natureneuroscience/>.

Reprints and permissions information is available online at <http://www.nature.com/reprints/index.html>.

- Jan, Y.N. & Jan, L.Y. Branching out: mechanisms of dendritic arborization. *Nat. Rev. Neurosci.* **11**, 316–328 (2010).
- Grueber, W.B. & Sagasti, A. Self-avoidance and tiling: mechanisms of dendrite and axon spacing. *Cold Spring Harb. Perspect. Biol.* **2**, a001750 (2010).
- Corty, M.M., Matthews, B.J. & Grueber, W.B. Molecules and mechanisms of dendrite development in *Drosophila*. *Development* **136**, 1049–1061 (2009).
- Hattori, D., Millard, S., Wojtowicz, W. & Zipursky, S. Dscam-mediated cell recognition regulates neural circuit formation. *Annu. Rev. Cell Dev. Biol.* **24**, 597–620 (2008).
- Hughes, M.E. *et al.* Homophilic Dscam interactions control complex dendrite morphogenesis. *Neuron* **54**, 417–427 (2007).
- Matthews, B.J. *et al.* Dendrite self-avoidance is controlled by Dscam. *Cell* **129**, 593–604 (2007).
- Matsubara, D., Horiuchi, S.Y., Shimono, K., Usui, T. & Uemura, T. The seven-pass transmembrane cadherin Flamingo controls dendritic self-avoidance via its binding to a LIM domain protein, Espinas, in *Drosophila* sensory neurons. *Genes Dev.* **25**, 1982–1996 (2011).
- Long, H., Ou, Y., Rao, Y. & van Meyel, D.J. Dendrite branching and self-avoidance are controlled by Turtle, a conserved IgSF protein in *Drosophila*. *Development* **136**, 3475–3484 (2009).
- Zipursky, S.L. & Sanes, J.R. Chemoaffinity revisited: dscams, protocadherins, and neural circuit assembly. *Cell* **143**, 343–353 (2010).
- Wadsworth, W.G., Bhatt, H. & Hedgecock, E. Neuroglia and pioneer neurons express UNC-6 to provide global and local netrin cues for guiding migrations in *C. elegans*. *Neuron* **16**, 35–46 (1996).
- Serafini, T. *et al.* The netrins define a family of axon outgrowth-promoting proteins homologous to *C. elegans* UNC-6. *Cell* **78**, 409–424 (1994).
- Mitchell, K.J. *et al.* Genetic analysis of Netrin genes in *Drosophila*: Netrins guide CNS commissural axons and peripheral motor axons. *Neuron* **17**, 203–215 (1996).
- Hiramoto, M., Hiromi, Y., Giniger, E. & Hotta, Y. The *Drosophila* Netrin receptor Frazzled guides axons by controlling Netrin distribution. *Nature* **406**, 886–889 (2000).
- Keleman, K. & Dickson, B. Short- and long-range repulsion by the *Drosophila* Unc5 netrin receptor. *Neuron* **32**, 605–617 (2001).
- Colon-Ramos, D.A., Margeta, M. & Shen, K. Glia promote local synaptogenesis through UNC-6 (netrin) signaling in *C. elegans*. *Science* **318**, 103–106 (2007).
- Teichmann, H.M. & Shen, K. UNC-6 and UNC-40 promote dendritic growth through PAR-4 in *Caenorhabditis elegans* neurons. *Nat. Neurosci.* **14**, 165–172 (2010).
- Park, J. *et al.* A conserved juxtacrine signal regulates synaptic partner recognition in *Caenorhabditis elegans*. *Neural Develop.* **6**, 28 (2011).
- Chan, S.S. *et al.* UNC-40, a *C. elegans* homolog of DCC (Deleted in Colorectal Cancer), is required in motile cells responding to UNC-6 netrin cues. *Cell* **87**, 187–195 (1996).
- Leonardo, E.D. *et al.* Vertebrate homologues of *C. elegans* UNC-5 are candidate netrin receptors. *Nature* **386**, 833–838 (1997).
- Smith, C.J. *et al.* Time-lapse imaging and cell-specific expression profiling reveal dynamic branching and molecular determinants of a multi-dendritic nociceptor in *C. elegans*. *Dev. Biol.* **345**, 18–33 (2010).
- Albeg, A. *et al.* *C. elegans* multi-dendritic sensory neurons: morphology and function. *Mol. Cell Neurosci.* **46**, 308–317 (2010).
- Oren-Suissa, M., Hall, D.H., Treinin, M., Shemer, G. & Podbilewicz, B. The fusen gene EFF-1 controls sculpting of mechanosensory dendrites. *Science* **328**, 1285–1288 (2010).
- Hall, D.H. & Treinin, M. How does morphology relate to function in sensory arbors? *Trends Neurosci.* **34**, 443–451 (2011).
- Aguirre-Chen, C., Bülow, H.E. & Kaprielian, Z. *C. elegans* bicd-1, homolog of the *Drosophila* dynein accessory factor Bicaudal D, regulates the branching of PVD sensory neuron dendrites. *Development* **138**, 507–518 (2011).
- Ishii, N., Wadsworth, W., Stern, B., Culotti, J. & Hedgecock, E. UNC-6, a laminin-related protein, guides cell and pioneer axon migrations in *C. elegans*. *Neuron* **9**, 873–881 (1992).
- Schwarz, V., Pan, J., Voltmer-Irsch, S. & Hutter, H. IgCAMs redundantly control axon outgrowth in *Caenorhabditis elegans*. *Neural Develop.* **4**, 13 (2009).
- Adler, C.E., Fetter, R. & Bargmann, C. UNC-6/Netrin induces neuronal asymmetry and defines the site of axon formation. *Nat. Neurosci.* **9**, 511–518 (2006).
- Watson, J.D. *et al.* Complementary RNA amplification methods enhance microarray identification of transcripts expressed in the *C. elegans* nervous system. *BMC Genomics* **9**, 84 (2008).
- Xu, Z., Li, H. & Wadsworth, W. The roles of multiple UNC-40 (DCC) receptor-mediated signals in determining neuronal asymmetry induced by the UNC-6 (netrin) ligand. *Genetics* **183**, 941–949 (2009).
- Yang, L., Garbe, D. & Bashaw, G. A frazzled/DCC-dependent transcriptional switch regulates midline axon guidance. *Science* **324**, 944–947 (2009).
- Tsalik, E.L. & Hobert, O. Functional mapping of neurons that control locomotory behavior in *Caenorhabditis elegans*. *J. Neurobiol.* **56**, 178–197 (2003).
- Eastman, C., Horvitz, H.R. & Jin, Y. Coordinated transcriptional regulation of the unc-25 glutamic acid decarboxylase and unc-47 GABA vesicular transporter by the *Caenorhabditis elegans* UNC-30 homeodomain protein. *J. Neurosci.* **19**, 6225–6234 (1999).
- Leung-Hageteijn, C. *et al.* UNC-5, a transmembrane protein with immunoglobulin and thrombospondin type 1 domains, guides cell and pioneer axon migrations in *C. elegans*. *Cell* **71**, 289–299 (1992).
- Killeen, M. *et al.* UNC-5 function requires phosphorylation of cytoplasmic tyrosine 482, but its UNC-40-independent functions also require a region between the ZU-5 and death domains. *Dev. Biol.* **251**, 348–366 (2002).
- Asakura, T., Ogura, K. & Goshima, Y. UNC-6 expression by the vulval precursor cells of *Caenorhabditis elegans* is required for the complex axon guidance of the HSN neurons. *Dev. Biol.* **304**, 800–810 (2007).
- Bashaw, G.J. & Goodman, C.S. Chimeric axon guidance receptors: the cytoplasmic domains of slit and netrin receptors specify attraction versus repulsion. *Cell* **97**, 917–926 (1999).
- Gitai, Z., Yu, T., Lundquist, E., Tessier-Lavigne, M. & Bargmann, C. The netrin receptor UNC-40/DCC stimulates axon attraction and outgrowth through enabled and, in parallel, Rac and UNC-115/AbLIM. *Neuron* **37**, 53–65 (2003).
- Hiramoto, M. & Hiromi, Y. ROBO directs axon crossing of segmental boundaries by suppressing responsiveness to relocalized Netrin. *Nat. Neurosci.* **9**, 58–66 (2006).
- Kuzina, I., Song, J.K. & Giniger, E. How Notch establishes longitudinal axon connections between successive segments of the *Drosophila* CNS. *Development* **138**, 1839–1849 (2011).
- Alexander, M. *et al.* An UNC-40 pathway directs postsynaptic membrane extension in *Caenorhabditis elegans*. *Development* **136**, 911–922 (2009).
- MacNeil, L., Hardy, W., Pawson, T., Wrana, J. & Culotti, J. UNC-129 regulates the balance between UNC-40 dependent and independent UNC-5 signaling pathways. *Nat. Neurosci.* **12**, 150–155 (2009).
- Merz, D.C., Zheng, H., Killeen, M.T., Krizus, A. & Culotti, J.G. Multiple signaling mechanisms of the UNC-6/netrin receptors UNC-5 and UNC-40/DCC *in vivo*. *Genetics* **158**, 1071–1080 (2001).
- Chang, C. *et al.* MIG-10/lamellipodin and AGE-1/PI3K promote axon guidance and outgrowth in response to slit and netrin. *Curr. Biol.* **16**, 854–862 (2006).
- Quinn, C.C., Pfeil, D. & Wadsworth, W. CED-10/Rac1 mediates axon guidance by regulating the asymmetric distribution of MIG-10/lamellipodin. *Curr. Biol.* **18**, 808–813 (2008).
- Fleming, T. *et al.* The role of *C. elegans* Ena/VASP homolog UNC-34 in neuronal polarity and motility. *Dev. Biol.* **344**, 94–106 (2010).
- Grueber, W.B. & Sagasti, A. Self-avoidance and tiling: mechanisms of dendrite and axon spacing. *Cold Spring Harb. Perspect. Biol.* **2**, a001750 (2010).
- Emoto, K., Parrish, J., Jan, L. & Jan, Y.-N. The tumour suppressor Hippo acts with the NDR kinases in dendritic tiling and maintenance. *Nature* **443**, 210–213 (2006).

## ONLINE METHODS

**Nematode strains and genetics.** The wild-type *C. elegans* Bristol strain N2 was used for all experiments and cultured as previously described<sup>48</sup>.

Mutants used in this study: *unc-6(ev400)*, *unc-6(rh46)*, *unc-5(e152)*, *unc-40(e271)*, *unc-129(ev554)*, *slt-1(eh15)*, *sax-3(ky123)*, *vab-2(ju1)*, *ptp-3(ok244)*, *madd-2(ok2266)*, *nid-1(cg119)*. Some strains were provided by the Caenorhabditis Genetics Center. All studies in this work used *C. elegans* hermaphrodites.

Additional strains:

NC1686 [*wIs51* (*F49H12.4::GFP + unc-119*)]<sup>20</sup>

NC1687 [*wIs52* (*F49H12.4::GFP + unc-119*)]<sup>20</sup>

CX6488 [*kyIs299, hsp16.2::unc-6::HA + odr-1::RFP*]<sup>27</sup>

YC149 [*unc-6(ev400); gIs9(unc-6::venus + odr-1::RFP)*]<sup>35</sup>

CZ1200 [*juIs76(unc-25::GFP)*]

NW1454 [*unc-5(e53); dpy-20(e1282); evIs105(pU5::HAAZU-5 + dpy-20(+))*]<sup>34</sup>

NW1151 [*unc-5(e53); evIs906(pU5::HAIG(N) + dpy-20(+))*]<sup>34</sup>

NW1180 [*unc-5(e53); evIs91(pU5::HAAZ-D + dpy-20(+))*]<sup>34</sup>

NW1137 [*unc-5(e53); evIs886(pU5::HA + dpy-20(+))*]<sup>34</sup>

Transgenic strains generated by microinjection:

NC2099 [*pha-1(e2123ts); wdEx682(MVC119(rig-3::unc-6) + pBx(pha-1(+ plasmid) + dat-1::mcherry))*]

NC2099 [*pha-1(e2123ts); wdEx682(MVC119(rig-3::unc-6) + pBx + dat-1::mcherry)*]

NC2182 [*pha-1(e2123ts); wdEx692(pCJS28, F49H12.4::unc-6::HA + pBx + dat-1::mcherry)*]

NC1893 [*pha-1(e2132ts); wdEx640(F49H12.4::unc-40::mcherry + pBx + odr-1::mcherry)*]

NC2059 [*pha-1(e2123ts); wdEx662(pCJS52(ser2prom3::unc-40::mcherry) + pBx + dat-1::mcherry)*]

NC2098 [*pha-1(e2123ts); wdEx681(pCJS68(unc-25::unc-40::mRFP) + pBx + dat-1::mcherry)*]

TV1788 [*unc-40(e271); wyls45; wyEx650(unc-40 minigene with mcherry injected at 20 ng/μl has co-selector marker GFP in coelomocytes)*]

NC2301 [*pha-1(e2123ts); wdEx746(pCJS93, F49H12.4::unc-40::GFP + pBx + pCJS85, dat-1::mcherry)*]

N2315 [*pha-1(e2123ts); wdEx748(pCJS98, F49H12.4::unc-40ΔECTO::mcherry + dat-1::mcherry + pBx)*]

NC2044 [*pha-1(e2123ts); wdEx660(pCJS65(unc-5::unc-5::CFP) + dat-1::mcherry + pBx)*]

NC2247 [*pha-1(e2123); lon-2(e678); wdEx716(pCJS72, unc-25::unc-5::mRFP + dat-1::mcherry + pBx)*].

**Molecular biology.** UNC-40, UNC-6 and UNC-5 expression plasmids were constructed using conventional cloning and gateway recombinase technology as previously described<sup>10,27,33,49</sup>. Detailed descriptions of plasmid constructs are available on request.

**Confocal microscopy.** Nematodes were immobilized with 15 mM levamisole on a 2% agarose pad in M9 buffer<sup>20</sup>. Images were obtained in a Leica TCS SP5 confocal microscope. z-stacks were collected with either 40× (1 μm/step), 63× (0.75 μm/step) or 100× (0.75 μm/step) objectives; single plane projections

were generated with Leica Application Suite Advanced Fluorescence software. Brightness and contrast were enhanced using Adobe Photoshop CS5.

**Time-lapse imaging.** Nematodes were imaged as previously described<sup>20</sup>. For each time point, the 40×, 63× or 100× objective was used to collect a z-stack (0.75 μm/step) spanning the focal depth of the PVD neuron and its dendritic branches. Dendritic branch outgrowth at each time point was evaluated from a z-projection. Larval stages were identified from morphological features: L2, postdeirid; L3, L4 and young adult, vulval development<sup>50</sup>. At least three independent movies verified each example of dynamic dendritic growth described in this report.

**Measuring 3° dendrite length.** Images from L4 larval worms were measured using the vector tool in ImageJ.

**Scoring self-avoidance defects.** Each genotype was visualized in a PVD::GFP reporter line (*wIs51* or *wIs52*). At least 20 worms (≥600 3° gaps) were visualized for each genotype. Confocal images were collected with a 40× objective in a z-stack to span the depth of PVD with a step size of 1 μm. PVD morphology was scored from z-stack projections. A self-avoidance defect was identified as any two adjacent 3° branches that lacked an intervening gap. Adjacent 3° branches were defined as physically linked to 2° branches projecting from flanking locations on the PVD 1° branch. The number of self-avoidance errors (that is, absence of intervening space between 3° branches of adjacent menorahs) was divided by the total number of potential 3° branch gaps per worm (that is, number of 2° branches – 2) to provide the fraction of overlapping 3° branches per worm. The average fraction of overlapping 3° branches for each genotype was calculated for histograms summarizing these results.

**Statistical analysis.** An unpaired Student's *t*-test was used to calculate statistical significance.

**Heat shock experiments.** Worms were heat shocked at the appropriate age as previously described<sup>27</sup>. All worms were imaged at the late L4 larval stage, after PVD development is complete.

**Temporal requirement for UNC-6.** *unc-6(rh46)* worms were maintained at the appropriate temperature<sup>29</sup> and treated with hypochlorite to release embryos for overnight incubation in M9 buffer. Synchronized L1 worms were placed on a bacterial lawn to initiate larval development and then shifted to either the permissive (15 °C) or restrictive (25 °C) temperature at specific larval intervals (L2/L3 larval transition, L3/L4 larval transition, end of L4 larval stage) for growth until the late young adult stage for imaging. Worms grown at either the permissive or restrictive temperature throughout development were used as controls.

48. Brenner, S. The genetics of *Caenorhabditis elegans*. *Genetics* **77**, 71–94 (1974).

49. Poon, V.Y., Klassen, M. & Shen, K. UNC-6/netrin and its receptor UNC-5 locally exclude presynaptic components from dendrites. *Nature* **455**, 669–673 (2008).

50. Sulston, J.E. & Horvitz, H. Post-embryonic cell lineages of the nematode, *Caenorhabditis elegans*. *Dev. Biol.* **56**, 110–156 (1977).